Enteric glia protect against *Shigella flexneri* invasion in intestinal epithelial cells: a role for *S*-nitrosoglutathione

Mathurin Flamant,[1,2,3] Philippe Aubert,[1,2,3] Malvyne Rolli-Derkinderen,[4] Arnaud Bourreille,[1,2,3] Margarida Ribeiro Neunlist,[1,2,3] Maxime M Mahé,[1,2,3] Guillaume Meurette,[1,2] Benoit Marteyn,[5] Tor Savidge,[6] Jean Paul Galmiche,[1,2,3] Philippe J Sansonetti,[5] Michel Neunlist[1,2,3]

See Commentary, p 429

► An additional material is published online only. To view this file please visit the journal online (http://gut.bmj.com).

[1]INSERM, UMR 913, Nantes, France
[2]CHU Nantes, Hôtel Dieu, Institut des Maladies de l'Appareil Digestif, Nantes, France
[3]Université de Nantes, Faculté de Médecine, Nantes, France
[4]INSERM, UMR 915, Nantes, France
[5]Unité de Pathogénie Microbienne Moléculaire & Unité INSERM 786, Institut Pasteur, Paris, France
[6]University Texas Medical Branch (UTMB), Department of Gastroenterology, Galveston, Texas, USA

Correspondence to
Dr Michel Neunlist, INSERM U913, Place Alexis Ricordeau, 44035 Nantes Cedex, France; michel.neunlist@univ-nantes.fr

Revised 21 October 2010
Accepted 25 October 2010
Published Online First 7 December 2010

ABSTRACT

Background Enteric glial cells (EGCs) are important regulators of intestinal epithelial barrier (IEB) functions. EGC-derived *S*-nitrosoglutathione (GSNO) has been shown to regulate IEB permeability. Whether EGCs and GSNO protect the IEB during infectious insult by pathogens such as *Shigella flexneri* is not known.

Methods *S flexneri* effects were characterised using in vitro coculture models of Caco-2 cells and EGCs (or GSNO), ex vivo human colonic mucosa, and in vivo ligated rabbit intestinal loops. The effect of EGCs on *S flexneri*-induced changes in the invasion area and the inflammatory response were analysed by combining immunohistochemical, ELISA and PCR methods. Expression of small G-proteins was analysed by western blot. Expression of ZO-1 and localisation of bacteria were analysed by fluorescence microscopy.

Results EGCs significantly reduced barrier lesions and inflammatory response induced by *S flexneri* in Caco-2 monolayers. The EGC-mediated effects were reproduced by GSNO, but not by reduced glutathione, and pharmacological inhibition of pathways involved in GSNO synthesis reduced EGC protecting effects. Furthermore, expression of Cdc42 and phospho-PAK in Caco-2 monolayers was significantly reduced in the presence of EGCs or GSNO. In addition, changes in ZO-1 expression and distribution induced by *S flexneri* were prevented by EGCs and GSNO. Finally, GSNO reduced *S flexneri*-induced lesions of the IEB in human mucosal colonic explants and in a rabbit model of shigellosis.

Conclusion These results highlight a major protective function of EGCs and GSNO in the IEB against *S flexneri* attack. Consequently, this study lays the scientific basis for using GSNO to reduce barrier susceptibility to infectious or inflammatory challenge.

Significance of this study

What is already known about this subject?
- Association between intestinal epithelial barrier (IEB) dysfunction and infectious or inflammatory diseases.
- Regulation of IEB functions (paracellular permeability, intestinal epithelial cell proliferation) by enteric glial cells (EGCs).
- Involvement of *S*-nitrosoglutathione (GSNO) in the control of paracellular permeability by EGCs.

What are the new findings?
- Demonstration of a specific protective role of EGCs during bacterial invasion.
- Identification of GSNO as a major glial mediator involved in IEB protection.
- Modulation of key proteins involved in *S flexneri* invasion by EGCs and GSNO.
- Ex vivo and in vivo validation in human and rabbit intestine, respectively.

How might it impact on clinical practice in the foreseeable future?
- As GSNO is already used in clinical trials (cystic fibrosis, prevention of cerebral ischaemia, treatment of pulmonary hypertension), this study could lay the scientific basis for its use in the treatment/prevention of gastrointestinal disorders associated with IEB dysfunction, in particular during infectious diseases.

INTRODUCTION

Emerging concepts suggest that defects in intestinal epithelial barrier (IEB) function, combined or not with altered immune function, are involved in the development of various digestive and non-digestive diseases.[1] In particular, the reduced ability of the IEB to resist pathogenic attack or to be repaired after attack has been associated with increased risk of developing infectious or inflammatory bowel diseases.[2] Therefore, approaches aimed at reinforcing IEB integrity could be of therapeutic interest, in both the prevention and treatment of these pathologies. Indeed, in a recent study, pharmacological reduction of intestinal permeability by blockage of tight junctions has been shown to attenuate intestinal inflammation in IL10−/− mice.[3] Similarly, enhancement of IEB tight junction expression and resistance with vasoactive intestinal peptide[4] reduced IEB lesions induced by pathogens such as *Citrobacter rodentium*.[5]

Various cellular or environmental components of the IEB have been shown to reinforce barrier functions. In particular, the enteric nervous system has recently been identified as a novel and major regulator of IEB functions. The enteric nervous system is an integrative neuronal network located along the gut and is composed of two major cell types, enteric neurons and enteric glial cells (EGCs).

EGCs outnumber enteric neurons by a factor of 4–10[6] and share common markers and properties with astrocytes of the central nervous system, which are known to regulate the blood–brain barrier. Recent studies have shown that EGCs can directly regulate various IEB functions. Indeed, EGCs inhibit intestinal epithelial cell (IEC) proliferation and reduce IEB permeability via the liberation of glial-derived transforming growth factor β1 and *S*-nitrosoglutathione (GSNO), respectively.[7 8] Interestingly, EGC lesions in animal models lead to disruption of IEB integrity followed by the development of jejunoileitis.[9 10] Moreover, glial disruption induces changes in the neurochemical coding of enteric neurons, which may partly be responsible for intestinal motility and permeability dysfunction.[11] However, whether EGCs can directly protect the IEB during pathophysiological stress and the nature of the glial-derived factors involved remain unknown.

Shigella flexneri is a major enteroinvasive pathogen that is responsible for bacillary dysentery, which accounts for over 100 million deaths world wide.[12] The physiopathological mechanisms have been identified using in vivo animal models and in vitro approaches. Shigellosis leads to destruction of the intestinal epithelium and a major intestinal inflammatory response.[13 14] More recently, using an ex vivo model of human colonic mucosa, we have shown that S *flexneri* induces major IEB lesions characterised by epithelial desquamation as early as 3 hours after infection, independently of the recruitment of the immune system.[15] Treatment of shigellosis includes an effective antibiotic, rehydration therapy and appropriate feeding during and after the episode of shigellosis. Prevention strategies have also been developed such as vaccination against the more important circulating strains and simple hand washing.[16] Whether strategies aimed at increasing barrier resistance to prevent the development of shigellosis would be effective is not known.

Therefore, our study aimed to determine the effect of EGCs and glial-derived GSNO on IEB resistance to attack by a clinically relevant pathogen, ie *S flexneri*. GSNO is the nitrosylated form of reduced glutathione (GSH), which has been shown to be produced by EGCs.[8 17] Nitrosylation of GSH is catalysed by caeruloplasmin, which therefore contributes to an antioxidant cytoprotective action.[18] Combining coculture models of EGCs and Caco-2 cells with in vivo and ex vivo approaches, we showed that EGCs and EGC-conditioned medium (EGC-CM) prevented the IEB lesions and inflammatory response induced by *S flexneri*. Finally, we identified glial-derived GSNO as a key mediator of these protective effects.

METHODS

Strains of *S flexneri*

Two strains of *S flexneri* (Institut Pasteur, Paris, France) were used in the study: (1) the wild-type *S flexneri* 5a M90T (INV+), which harbours a virulence plasmid encoding its invasive phenotype; (2) the plasmid-cured mutant non-invasive strain BS176 (INV−). The two strains were stored at 4°C on Petri dishes containing 30 ml Bacto Agar (Becton Dickinson, Le Pont de Claix, France) supplemented with 0.01% of Congo red (Merck, Darmstadt, Germany). Sixteen hours before experiments, one colony of INV+ or INV− strain was suspended in 10 ml Bacto Agar broth and cultured overnight at 37°C. Bacteria were then adjusted to 10^9 colony forming units (CFU)/ml by absorbance measurement at 600 nm with a Varioscan microplate reader (Thermo, Courtaboeuf, France). The culture media were centrifuged (10 min/2500 rpm), resuspended in Bacto Agar broth (10 ml), diluted 1:10 in the same medium (10 ml), and then cultured for 2 h before their use in the exponential phase of growth for experiments. Bacteria were centrifuged (10 min/2500 rpm) and resuspended in Dulbecco's modified Eagle's medium (DMEM) (without antibiotics).

Culturability of *S flexneri*

S flexneri was cultured in the presence of GSNO (50 μM) or EGC-CM (1:2 dilution) for 30 min, 1 h, 2 h or 3 h. Appropriate dilutions (from 10^{-4} to 10^{-6}) of *S flexneri* were performed, and CFU were quantified by spread plate counts on Bacto Agar (from 30 to 300 colonies per plate). Plates were incubated for 24 h at 37°C. The assessment of culturability was systematically based on the results of three independent samples.

Rabbit intestinal loop infection with *S flexneri*

Six New Zealand White rabbits, weighing 2.5–3.0 kg (Charles River Laboratories, St Aubin les Elbert, France), were used in this study. Animals were fasted for 24 h before being infected, and all manipulations were performed under general anaesthesia after intravenous injection of 6% sodium pentobarbital (0.5 ml/kg). After a laparotomy, ligated ileal loops (5 cm long) were made; ligations were carefully performed to preserve the afferent and efferent mesenteric musculature. In each loop, 0.5 ml of a bacterial suspension containing 10^9 bacteria was injected. The abdominal cavity was then closed, and the animals were killed 8 h later. Intraperitoneal injection of GSNO (6 mM final concentration in 50 mM Hepes, pH 7.4, 10 ml) was performed through a catheter. The initial dose was injected 30 min after ligation, and then 2 h, 4 h and 6 h after infection. Control animals were injected under similar conditions with saline solution (0.9% NaCl). In each rabbit, seven loops were ligated, five for *S flexneri* (INV+) injection and two for Hepes injection. After fixation in paraformaldehyde, tissues were washed in phosphate-buffered saline (PBS), dehydrated and embedded in paraffin. Sequential sections of mucosa (5 μm) were cut. Infected and control tissues were observed by classic microscopy after H&E staining. Each section was observed under an Olympus IX 50 microscope. Pictures were acquired with a black and white video camera (Mod4910, Cohu Inc; SL Microtest, Jena, Germany) connected to a Macintosh computer through a frame-grabber card (Scion Image; SL Microtest). Four parameters were analysed as previously described.[19]

a. Length/width ratio (L/W) of the villus reflecting villous atrophy: 40 villi were analysed on each section, their length and width were recorded, and the ratio calculated. As seven loops were performed for each rabbit, the mean value was therefore computed on a total of 200 villi for infected INV+ loops and 80 villi for control loops.
b. Ratio between thickness of the submucosa and thickness of the submucosa + length of the villus and crypt (SM/SM+L), reflecting the intensity of submucosal oedema. The mean of 40 ratios for each section was therefore calculated.
c. Percentage of villi with ulceration.
d. Number of polymorphonuclear leucocytes (PMNLs) invading the tissue. On each of the 40 intestinal villi examined on each section, PMNLs were counted at two levels as previously described: in the crypt area and in the villus area. Again, the mean was calculated from a total of 200 villi for infected loops and 80 for control loops.

Organotypic culture model

Tissue specimens were obtained from patients who underwent surgery for colonic adenocarcinoma, according to the guidelines of the French Ethics Committee for Research on Human Tissues. None of these patients received chemotherapy or non-steroidal

anti-inflammatory drugs before surgery. Specimens were taken at a distance from the tumour in macroscopically and histologically normal areas and immediately processed in the pathology department. According to the guidelines of the French Ethics Committee for Research on Human Tissues, these specimens were considered to be 'residual tissue', not relevant to pathological diagnosis. All specimens were collected before August 2007. At that time, the specimens considered as 'residual tissue' did not require patient consent. Tissue samples were placed in oxygenated sterile Krebs solution containing 117 mM NaCl, 4.7 mM KCl, 1.2 mM $MgCl_2$,$6H_2O$, 1.2 mM NaH_2PO_4, 25 mM $NaHCO_3$, 2.5 mM $CaCl_2$,$2H_2O$ and 11 mM $C_6H_{12}O_6$ (glucose), and then rapidly transported to the laboratory for experiments. Colonic fragments were pinned down with the mucosa in a sterile Sylgard-coated dish containing oxygenated sterile Krebs solution maintained at 4°C and changed every 10 min. Muscle layers were removed under a dissection microscope (Olympus, Rungis, France). After dissection of the muscle layers, the tissue was turned over and pinned flat with the mucosa up. Equal-sized fragments (1 cm×1 cm) of both the mucosa and submucosa were washed four times with sterile Krebs solution, weighed, and then pinned in a Sylgard-coated sterile dish. The specimens were then maintained in short-term organ culture for 30 min in DMEM (supplemented with 10% heat-inactivated fetal calf serum (FCS) and 2 mM glutamine) alone or supplemented with EGC-CM (1:2 dilution) or GSNO (50 μM). The invasive strain of INV+ (adjusted to 10^9 CFU/ml by absorbance measurement at 600 nm with a Varioscan microplate reader) or no bacteria (control tissues) was added to the medium for 3 h. The culture medium was removed after 3 h of infection and stored at −80°C. After fixation in paraformaldehyde (4%, 3 h at room temperature), tissues were washed in PBS, dehydrated, and embedded in paraffin. Sequential sections of mucosa (5 μm) were cut. Infected and control tissues were observed by classic microscopy after H&E staining. Stained tissue sections were observed with an Olympus IX 50 microscope (20× objective). Pictures were acquired with a black and white video camera as described above. Two parameters were analysed as previously described[15]: (*a*) the length of epithelial desquamation compared with the length of intact epithelium (%); (*b*) the height of the surface epithelium. The mean value was therefore computed on a total of 10 fields examined per experiment and per condition.

Cell lines

Caco-2 human adenocarcinoma cells (EATCC, Port Down, UK) were cultured in DMEM (4.5 g/l glucose) supplemented with 10% heat-inactivated FCS, 2 mM L-glutamine, 50 IU/ml penicillin and 50 μg/ml streptomycin at 37°C and 5% CO_2. All cell reagents were from Invitrogen (Cergy-Pontoise, France). Cells were seeded on to a porous filter (0.40 μm porosity, 1.1 cm diameter; Corning, Marne-la-Vallée, France) at a density of 2×10^5 cells/filter and grown to confluence (14 days). Porous filters were used for coculture experiments in 12-well plates (Corning, Avon, France). Culture medium was changed every 48 h.

Non-transformed and transformed EGCs were generated as previously described.[20] EGC cultures were isolated and purified from enzymatically dissociated preparations of rat longitudinal muscle/myenteric plexi. EGCs were cultured in DMEM (4.5 g/l glucose) supplemented with 10% heat-inactivated FCS, 2 mM L-glutamine, 50 IU/ml penicillin and 50 μg/ml streptomycin at 37°C and 5% CO_2. EGCs were seeded at a density of 1.5×10^5 cells in the bottom of 12-well plates (Corning) and grown to confluence (4 days) at 37°C and 5% CO_2. For some experiments, EGC-CM was collected, centrifuged and stored at −80°C until used as a conditioned medium.

Human fibroblasts cells (CCD-18Co) were cultured in minimal essential medium supplemented with 10% heat-inactivated FCS, 2 mM L-glutamine, 0.1 mM non-essential amino acid, 50 IU/ml penicillin and 50 μg/ml streptomycin at 37°C and 5% CO_2. CCD-18Co cells were seeded at a density of 2×10^5 cells in the bottom of 12-well plates (Corning) and grown to confluence (7 days) at 37°C and 5% CO_2.

Coculture and infection

Monolayers of Caco-2 cells were cultured in the presence of cells seeded in the bottom of 12-well plates or with other components added to the culture medium in the bottom of the 12-well plates. All components of the coculture model were cultured with the culture medium for epithelial cells. After 90 min of infection of Caco-2 cells with *S flexneri*, gentamicin (50 μg/ml) was added to the apical side of the filters for 30 min to kill extracellular bacteria, allowing the study of invasive bacteria exclusively. Filters were then washed three times with DMEM, and Caco-2 cells were subsequently cocultured for 16 h.

Experiments were performed under different conditions: Caco-2 cells cultured alone or in the presence of EGCs, CCD-18Co cells (seeded at the bottom), EGC-CM (1:2 dilution), GSNO (10, 50, 100 μM; WPI, Aston Stevenage, UK) or GSH (10, 50, 100 μM; Sigma, Saint Quentin Fallavier, France). To inhibit endogenous nitric oxide synthetase activity, EGCs were incubated for 1 h before the experiment with N^G-nitro-L-arginine methyl ester (L-NAME; 50 μM; Interchim, Montluçon, France). To reduce the GSNO secreted by EGCs, EGC-CM was incubated with dithiothreitol (DTT; 0.1 mM; Invitrogen) for 1 h before the experiment.Caco-2 cells and EGCs were cocultured 1 day before infection by *S flexneri* (INV+, INV−).

Intestinal epithelial monolayer permeability was evaluated by measuring transepithelial resistance (TER) using an EVOM resistance metre (WPI). The resistance was calculated by subtracting the electrical resistance of a blank insert from the measured value.

Morphological and immunohistochemical analysis

At the end of the experiment, filters of Caco-2 cells were fixed for 30 min in PBS containing 4% paraformaldehyde (Sigma) at room temperature. The filters were washed three times in PBS and permeabilised for 30 min in PBS/NaN_3 with 0.5% Triton X-100 (Sigma) and 4% horse serum (Sigma). Permeabilised Caco-2 cells were then exposed to a primary rabbit antibody anti-*S flexneri* (Flexner 5; 1:2000 dilution; from P Sansonetti, Institut Pasteur, Paris, France), mouse anti-ZO-1 (1:500 dilution; Clinisciences, Montrouge, France) or Alexa Fluor phalloidin fluorescein isothiocyanate (FITC; 1:200 dilution; Invitrogen) for 90 min at room temperature and washed three times with PBS. Caco-2 cells were thereafter incubated for 30 min with a secondary anti-rabbit antibody conjugated with CY3 (1:500 dilution; Becton Dickinson) and an anti-mouse antibody conjugated with CY5 (1:200 dilution; Becton Dickinson). Caco-2 cell monolayers were observed with an Olympus IX 50 fluorescence microscope (4× objective). Pictures were acquired with a black and white video camera as described above. Two parameters were analysed: (*a*) areas of immunostained sites of infection at 4, 8 and 16 h after invasion; (*b*) numbers of invasion foci at 8 and 16 h after invasion. The mean value was therefore computed on a total of 11 fields examined per experiment and per condition representing about 20% of the total area of the filter. ZO-1 expression and distribution as well as localisation of

INV+ were analysed with a confocal-like microscope Axiovert 200M coupled to an ApoTome (Zeiss, Gottingen, Germany).

Epithelial cytokine production

Apical and basolateral supernatants of cell cultures and organotypic culture were collected, and interleukin (IL)-8 (Becton Dickinson) protein concentration was determined using a commercially available ELISA kit according to the manufacturer's instructions. Each sample was assessed in duplicate. For determination of intracellular IL-8 concentration, the intracellular proteins were extracted using RIPA lysis buffer (Millipore, Saint Quentin en Yvelines, France) containing a protease inhibitor cocktail (Roche Diagnostics, Meylan, France) and measured by ELISA.

Real-time quantitative reverse transcriptase PCR

Total RNA was extracted from cells using RLT (Qiagen, Courtaboeuf, France) according to the manufacturer's instructions. Total RNA (5 μg), $pd(N)_6$ random hexamers (1 μl; 265 ng/μl; GE Healthcare, Orsay, France) dNTPs (1 μl; 10 mM; Gibco, Cergy-Pontoise, France), first-strand buffer 5X (5 μl; Gibco), DDT (1 μl; 0.1 M, Gibco) and RNasin (0.5 μl; 40 U/μl; Promega, Charbonnieres, France) were used to synthesise single-stranded cDNA using the Superscript II Reverse Transcriptase (0.5 μl; 200 U/μl; Invitrogen) according to the manufacturer's instructions, in a total volume of 25 μl. Incubation was performed at 42°C for 60 min. Amplification conditions for the IL-8 and S6 templates were optimised for the RotorGene 2000 instrument (Ozyme, Saint Quentin en Yvelines, France). PCRs were performed with 2 μl cDNA, 0.1 μl of a solution of SYBR Green I diluted 1:100 (Sigma), 1 μl (10 μM) of each primer, 1 μl (10 mM) dNTPs, and 0.4 μl Titanium Taq DNA polymerase kit (Ozyme), according to the manufacturer's instructions. Cycling conditions were as follows: 5 min at 95°C; amplification for 35 cycles with denaturation for 5 s at 95°C; annealing 15 s at 60°C for S6, 63°C for IL-8, and extension, 20 s at 72°C. Primers were chosen on separate exons to amplify cDNA but not genomic DNA. The following primers were used: S6 forward, 5′-CCAAGCTTATT CAGCGTCTTGTTACTCC-3′; reverse, 5′-CCCTCGAGTCCTT CATTCTCTTGGC-3′ (PCR product 130 bp); IL-8 forward, 5′-CTCTTGGCAGCCTTCCTGATT-3′; reverse, 5′-TATGCACT GACATCTAAGTTCTT-3′ (PCR product 264 bp). An external standard curve was generated with serial dilutions of control cDNA, by plotting the relative amounts of these dilutions against the corresponding C_t (threshold cycle) values. The amount of IL-8 and S6 was calculated from these standard curves using the RotorGene software (Ozyme). Samples were tested in triplicate, and the mean values were used for quantification using the $2^{-\Delta\Delta CT}$ method as previously described.[21]

Western blot analysis

After treatment, cells were harvested and homogenised in NETF lysis buffer containing 100 mM NaCl, 2 mM EGTA, 50 mM Tris/HCl, 50 mM NaF, 1% Nonidet P-40, 2 mM orthovanadate, protease inhibitor cocktail (Sigma), and serine–threonine phosphatase inhibitor cocktail (Sigma). Nuclei and unlysed cells were removed by centrifugation at 10 000 *g* for 10 min at 4°C. Proteins were resolved by sodium dodecyl sulfate/polyacrylamide gel electrophoresis and transferred to nitrocellulose membranes that were incubated with specific antibodies. Signals from immunoreactive bands were detected by ECLplus (General Electric) and quantified using QuantityOne (BioRad, Marnes-la-Coquette, France). Equal loading was checked by reprobing the membrane with monoclonal β-actin antibody (Sigma). Rabbit anti-phospho-PAK1/2 (phospho-PAK1(Ser199/204)/PAK2 (Ser 192/197), anti-PAK1, anti-Cdc42, anti RhoA, anti-MYPT and anti-Rac1 were purchased from TEBU Bio (Le Perray en Yvelines, France).

Statistical analysis

Each set of experiments (cell culture and tissue culture) was repeated at least three times. Data are expressed as mean±SEM. A paired t test, a Mann–Whitney U test, or a one-way or repeated major analysis of variance followed by Bonferroni t test were performed to compare different populations. Differences were considered significant at $p<0.05$.

RESULTS

Enteric glia directly protect Caco-2 monolayers during infectious stress

To determine the ability of EGCs to protect the IEB during infection by *S flexneri*, we used a validated coculture model of confluent Caco-2 cells grown on Transwell filters and EGCs.[4 8]

Enteric glia reduce intestinal barrier invasion by *S flexneri*

Incubation of Caco-2 monolayer with the invasive strain of *S flexneri* (INV+) induced a time-dependent increase in the surface area of the monolayer infected with INV+ (figure 1A,C,E). In addition, the number of infection foci increased in a time-dependent fashion (figure 1F). The non-invasive strain of *S flexneri* (INV−) did not infect Caco-2 monolayers (data not shown).

Coculture of Caco-2 monolayer with EGCs 24 h before and during infection with INV+ significantly reduced both the infected surface area and the number of infection foci compared with the control (ie, Caco-2 cells cultured alone infected with INV+) (figure 1B,D–F). Furthermore, preincubation alone of Caco-2 monolayer with EGCs before infection also significantly reduced the lesions induced by INV+ (figure 2A). In contrast, coculture of Caco-2 cells with EGCs only after infection with INV+ did not modify the extent of the lesions in the Caco-2 monolayer compared with the control (data not shown). Culture of Caco-2 monolayer with EGC-CM also significantly reduced monolayer lesions induced by INV+ (figure 2A).

To address the cell-specific effects of EGCs, we evaluated the protective effects of the human fibroblast cell line (CCD-18Co), as fibroblasts are another major cell component of the mucosa. After coculture of Caco-2 monolayer with CCD-18Co, infection by INV+ induced similar lesions to those observed in the control (figure 2B).

Enteric glia inhibit alterations in intestinal barrier resistance induced by INV+

Infection of Caco-2 monolayer with INV+ induced a significant time-dependent decrease in TER as early as 8 h after infection (figure 3A). In contrast, coculture of Caco-2 cells with EGCs did not modify TER during the first 8 h after infection. However, at 16 h after infection, there was a significant decrease in TER, which was, however, larger than that observed in the control (figure 3A). Interestingly, TER of the Caco-2 monolayer cocultured with EGCs was significantly larger than that of Caco-2 cells cultured alone, in both the absence and presence of INV+. In addition, INV− did not modify Caco-2 monolayer TER measured in the presence or absence of EGCs (data not shown).

Enteric glia inhibit the inflammatory response induced by INV+

Infection of Caco-2 monolayer with INV+ induced a time-dependent increase in IL-8 concentration compared with that

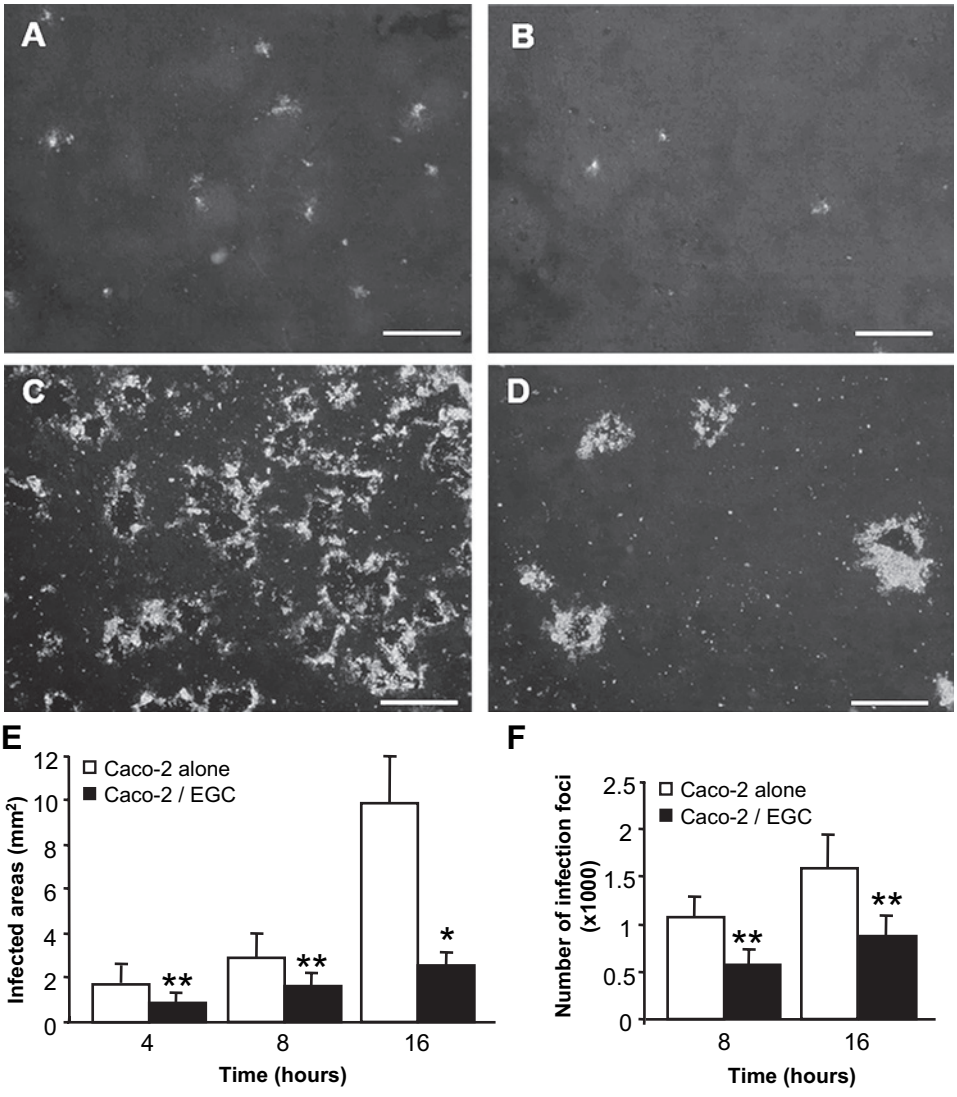

Figure 1 Intestinal epithelial barrier protection by enteric glia during attack by *S flexneri*. (A—D) Immunostaining of Caco-2 monolayer with an anti-Shigella antibody cultured without (A,C) or with (B,D) enteric glial cells (EGCs) 8 h (A,B) and 16 h (C,D) after infection with *S flexneri*. In the presence of EGCs, the infection area and number of foci are reduced compared with the controls. Scale bar: 250 μm. (E) Quantitative analysis of invasion areas by *S flexneri* in Caco-2 monolayer cultured alone and in the presence of EGCs (n=8, *p<0.05; **p<0.01). (F) Quantitative analysis of number of infection foci by *S flexneri* in Caco-2 cells cultured alone and in the presence of EGCs (n=8, **p<0.01).

measured in non-infected monolayers (figure 3B). This increase was significant as early as 4 h after infection. In addition, IL-8 concentrations were significantly higher in the basolateral than the apical compartment (figure 3B). Interestingly, 16 h after infection, IL-8 concentration correlated linearly with the total surface area of the infected monolayer infected with INV+ (r=0.96, p<0.05, n=5).

At all times measured, coculture of Caco-2 monolayer with EGCs significantly reduced INV+-induced IL-8 secretion on both the apical and basolateral side compared with the control (figure 3B). Interestingly, in Caco-2 cells, the ratio of intracellular stored IL-8 to the total secreted and stored IL-8 was significantly increased after culture with EGCs compared with the control (figure 3C).

Finally, at 4 h after infection, INV+ induced a significant increase in IL-8/S6 mRNA expression in Caco-2 cells compared with non-infected Caco-2 cells (figure 3D). In addition, IL-8/S6 mRNA expression level was significantly reduced in INV +-infected Caco-2 monolayer cultured with EGCs compared with the control (figure 3D).

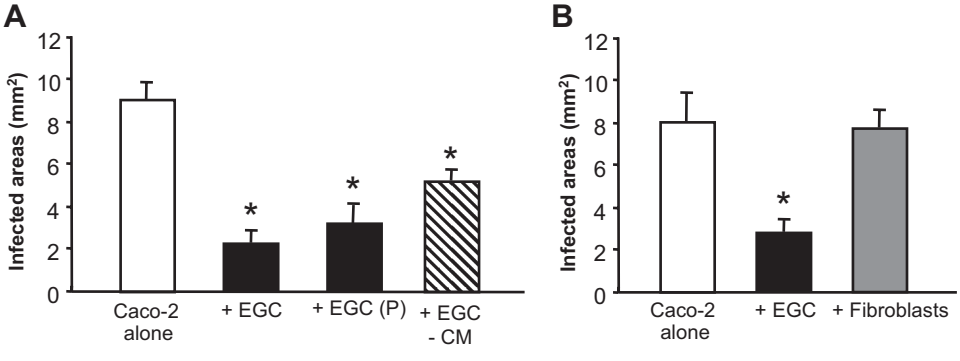

Figure 2 Intestinal epithelial barrier (IEB) protection by enteric glia but not fibroblasts during attack by *S flexneri*. (A) Preincubation of Caco-2 monolayer with enteric glial cells (EGCs) 24 h before infection (EGC(P)) was sufficient to protect IEB lesions induced by *S flexneri* (n=4, *p<0.05). In addition, EGC-conditioned medium (EGC-CM) prevented the Caco-2 monolayer invasion by *S flexneri* (n=4, *p<0.05). (B) A coculture model with fibroblasts did not reproduce the protective effects of EGCs in Caco-2 cells (n=4).

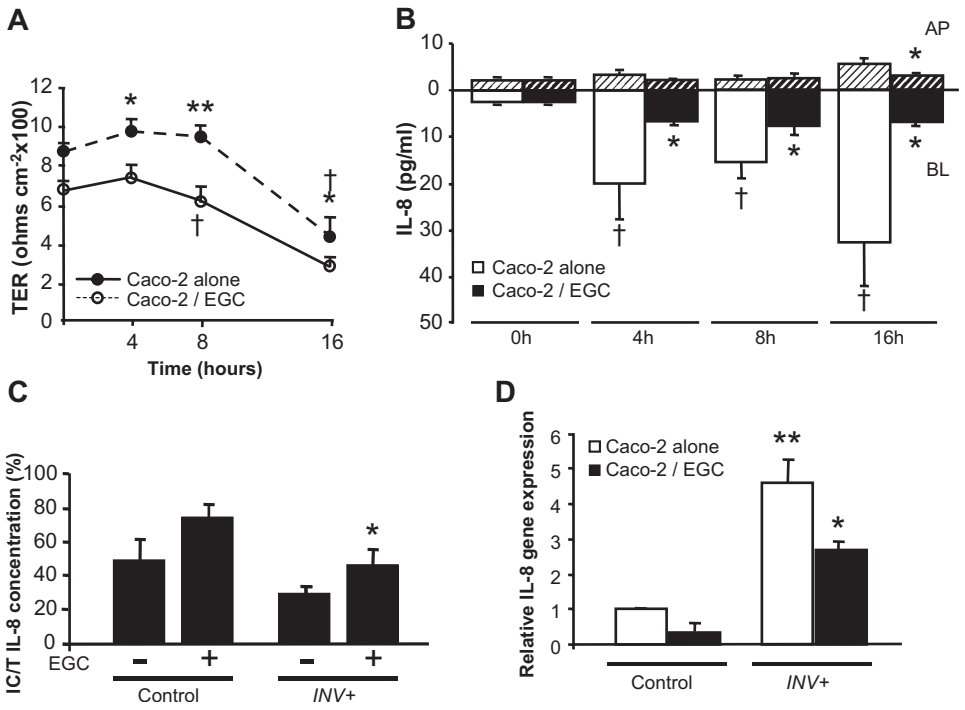

Figure 3 Modulation of intestinal epithelial barrier resistance and inflammatory response by enteric glial cells (EGCs) during attack by *S flexneri*. (A) Transepithelial resistance (TER) of Caco-2 cells after infection by *S flexneri* showed a significant decrease as early as 8 h after infection in Caco-2 cells alone but only at 16 h in the presence of EGCs (n=8, †p<0.05 compared with initial time of infection). In addition, TER was significantly increased in the presence of EGCs compared with Caco-2 cells alone (n=8, *p<0.05; **p<0.01). (B) Infection by *S flexneri* induced polarised interleukin (IL)-8 secretion at the basolateral (BL) side compared with the apical (AP) side. Secretion of IL-8 was decreased in the presence of EGCs compared with the control (n=8, *p<0.05, †p<0.05 compared with initial time of infection). (C) Ratio of intracellular/total (IC/T) IL-8 concentration in the Caco-2 monolayer. In the presence of EGCs, an increase in (IC/T) IL-8 ratio was observed (n=5, *p<0.05). (D) Relative IL-8 gene expression showing an increase in IL-8 mRNA after *S flexneri* infection compared with the control (n=5, †p<0.05). Coculture conditions led to a decrease in IL-8/S6 mRNA expression, which was induced compared with Caco-2 cells alone (n=5, *p<0.05).

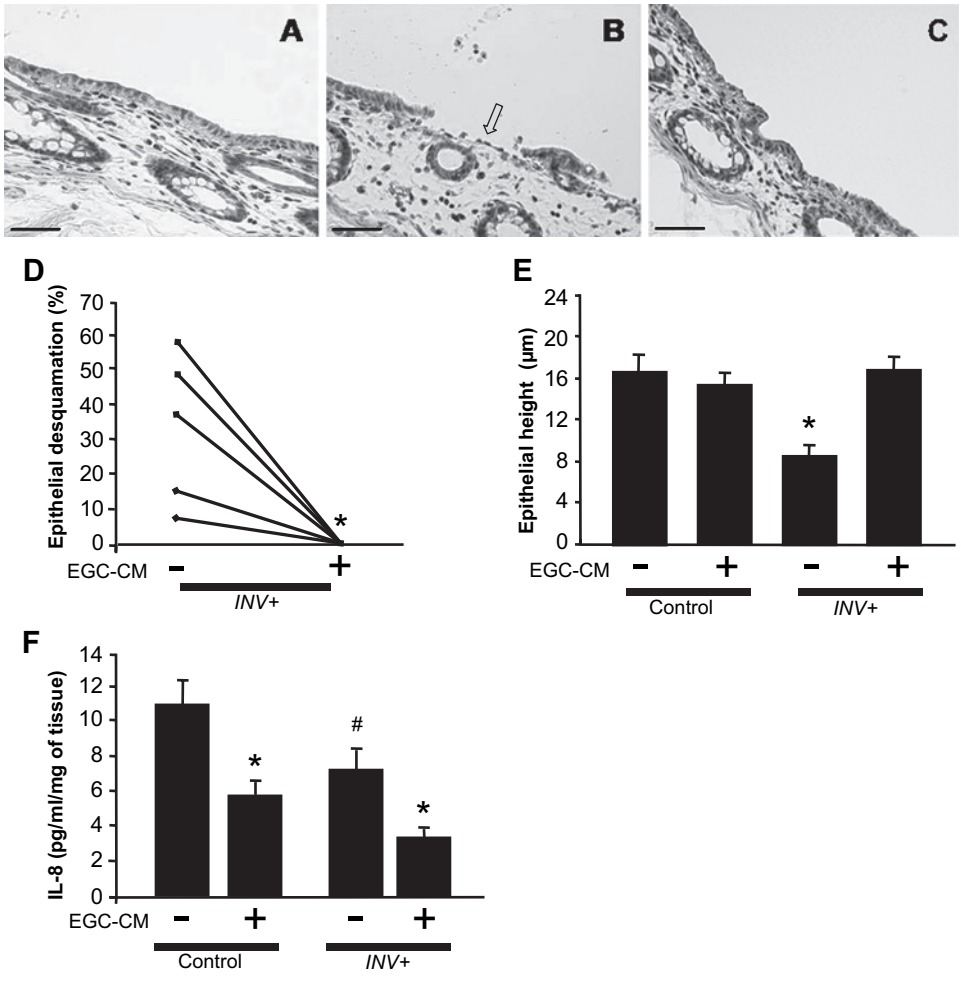

Figure 4 Modulation by enteric glial cell conditioned medium (EGC-CM) of *S flexneri* effects on barrier morphology and inflammatory response in human colonic explants. (A) No surface epithelium desquamation was observed in control non-infected colonic tissues cultured for 3 h. (B) Infection of the colonic specimen for 3 h with *S flexneri* induced significant desquamation of the surface epithelium (arrow). (C) In the presence of EGC-CM, no desquamation was observed. Scale bars: 50 µm. (D) Quantitative analysis of epithelial desquamation revealed that EGC-CM prevented the desquamation of the surface epithelium induced by *S flexneri* (INV+) (n=5, *p<0.05). (E) *S flexneri* (INV+) induced a significant decrease in surface epithelial height compared with non-infected tissues. EGC-CM prevented *S flexneri*-induced decrease in epithelial height (n=5, *p<0.05). (F) EGC-CM induced a significant decrease in interleukin (IL)-8 secretion compared with the control in both control and infected tissues (n=5, *p<0.05, #p<0.05 compared with the control condition without EGC-CM).

EGC-CM protects human colonic mucosa during infectious stress

To further validate the protective effects of EGCs during IEB infection by INV+, we used explants of human colonic mucosa as previously described.[15]

In the absence of infection, no epithelial damage was observed at the end of the 3 h of culture (figure 4A). Infection of human colonic mucosa explants by INV+ for 3 h induced significant desquamation of the surface epithelium (figure 4B,D). In contrast, in the presence of EGC-CM, no desquamation of surface epithelium was induced by INV+ (figure 4C,D). Moreover, infection of colonic explants by INV+ induced a significant decrease in epithelium height compared with the control, which was also prevented by EGC-CM (figure 4E). In addition, EGC-CM significantly reduced IL-8 concentration in infected colonic explants compared with the control (figure 4F). Interestingly, EGC-CM also reduced IL-8 concentration in non-infected colonic explants compared with the control (figure 4F).

Glial-derived GNSO mediates the protective effects of enteric glia during infectious insult

A recent study has identified GSNO as an enteric glial mediator involved in the EGC-induced increase in IEB resistance.[8] We therefore sought to determine whether GSNO could be involved in the EGC-mediated protection of the IEB.

GSNO reduces barrier lesions and inflammatory response induced by INV+

Incubation of Caco-2 monolayer with GSNO induced a bell-shaped dose-dependent reduction in the surface area of the monolayer infected with INV+ compared with the control (figure 5A). Maximum protective effect was obtained at 50 μM GSNO. Interestingly, GSH (10, 50 and 100 μM) did not protect INV+-induced lesions in Caco-2 monolayer (figure 5A). Preincubation alone of Caco-2 monolayer with GSNO for 24 h before infection was sufficient to prevent IEB lesions induced by INV+ (figure 5B). In addition, treatment of Caco-2 monolayer with GSNO significantly reduced the INV+-induced increase in polarised IL-8 secretion compared with the control (figure 5C).

To demonstrate that EGCs protect IEB via the production of GSNO, we inhibited its synthesis directly in EGCs using pharmacological approaches as previously described.[8] Blocking nitric oxide synthetase activity in EGCs, which is involved in GSNO synthesis from GSH, using L-NAME (50 μM), significantly inhibited the protective effects of EGCs (figure 6A). Pretreatment of EGC-CM with DTT (0.1 mM) also significantly prevented the protective effects of EGCs (figure 6B).

EGCs and GSNO do not affect *S flexneri* viability

We next determined whether EGCs or GSNO could modulate bacterial viability. Therefore, INV+ bacteria were cultured with EGC-CM for 3 h, and their culturability was quantified by spread plate counts. No difference in counts between INV+ cultured in the presence or absence of EGC-CM was observed. Similarly, no significant difference in counts was observed after incubation of INV+ in the presence or absence of GSNO (online supplementary files A and B). Furthermore, after pretreatment of INV+ with GSNO, INV+ tended to induce a larger infection area in Caco-2 monolayer than in the control (non-treated INV+) (online supplementary file C).

Effect of EGCs and GSNO on intestinal barrier and entry of *S flexneri*

Microscopy studies with an ApoTome revealed that INV+ bacteria were mainly localised within Caco-2 cells under control

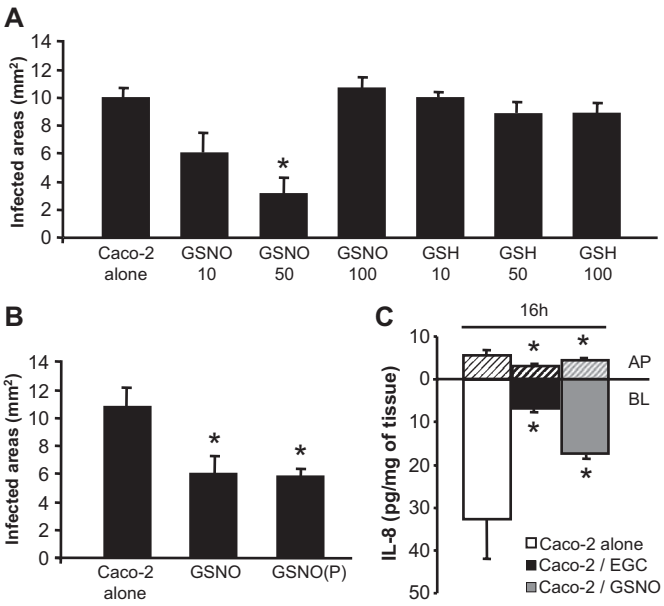

Figure 5 Intestinal epithelial barrier (IEB) protection by glial-derived *S*-nitrosoglutathione (GSNO) during attack by *S flexneri*. (A) GSNO but not reduced glutathione (GSH) induced a bell-shaped dose dependent reduction in the surface area of the monolayer infected with *S flexneri* (n=4, *p<0.05). (B) Preincubation of IEB before infection with GSNO (GSNO(P)) reproduced the protective effects of GSNO (n=4, *p<0.05). (C) GSNO and enteric glial cells (EGCs) significantly reduced polarised interleukin (IL)-8 secretion by IEB, at both the apical (AP) and basolateral (BL) side, induced by *S flexneri* (n=6, *p<0.05).

conditions (figure 7A). In contrast, after treatment with EGCs (figure 7B) or GSNO (figure 7C), INV+ was also observed within Caco-2 cells, but also frequently over the Caco-2 monolayer. Furthermore, INV+ induced a major reduction in the pericellular staining of ZO-1 in control Caco-2 monolayer (figure 7D) compared with the Caco-2 monolayer cocultured with EGCs (figure 7E) or GSNO (figure 7F). In addition, EGCs and GSNO prevented the irregular pericellular staining patterns of ZO-1 induced by INV+ in control Caco-2 monolayer (Figure 7D–F).

EGCs and GSNO reduce Cdc42 and phospho-PAK expression in epithelial cells

As Rho proteins are known to play a key role in bacterial invasion,[22 23] we evaluated the effect of EGCs or GSNO on RhoA or Cdc42 and Rac1 expression as well as their target

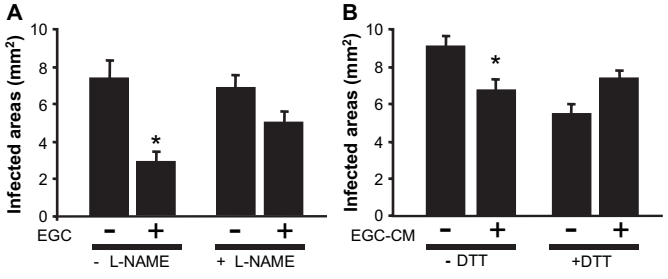

Figure 6 Intestinal epithelial barrier (IEB) protection by glial-derived *S*-nitrosoglutathione (GSNO) during attack by *S flexneri*. (A) The protective effect of enteric glial cells (EGCs) on the infected area of the IEB was abolished in the presence of N^G-nitro-L-arginine methyl ester (L-NAME; n=5, *p<0.05). (B) The protective effect of EGCs on the infected area of the IEB was abolished after treatment of EGC-conditioned medium (EGC-CM) with dithiothreitol (DTT; n=5, *p<0.05).

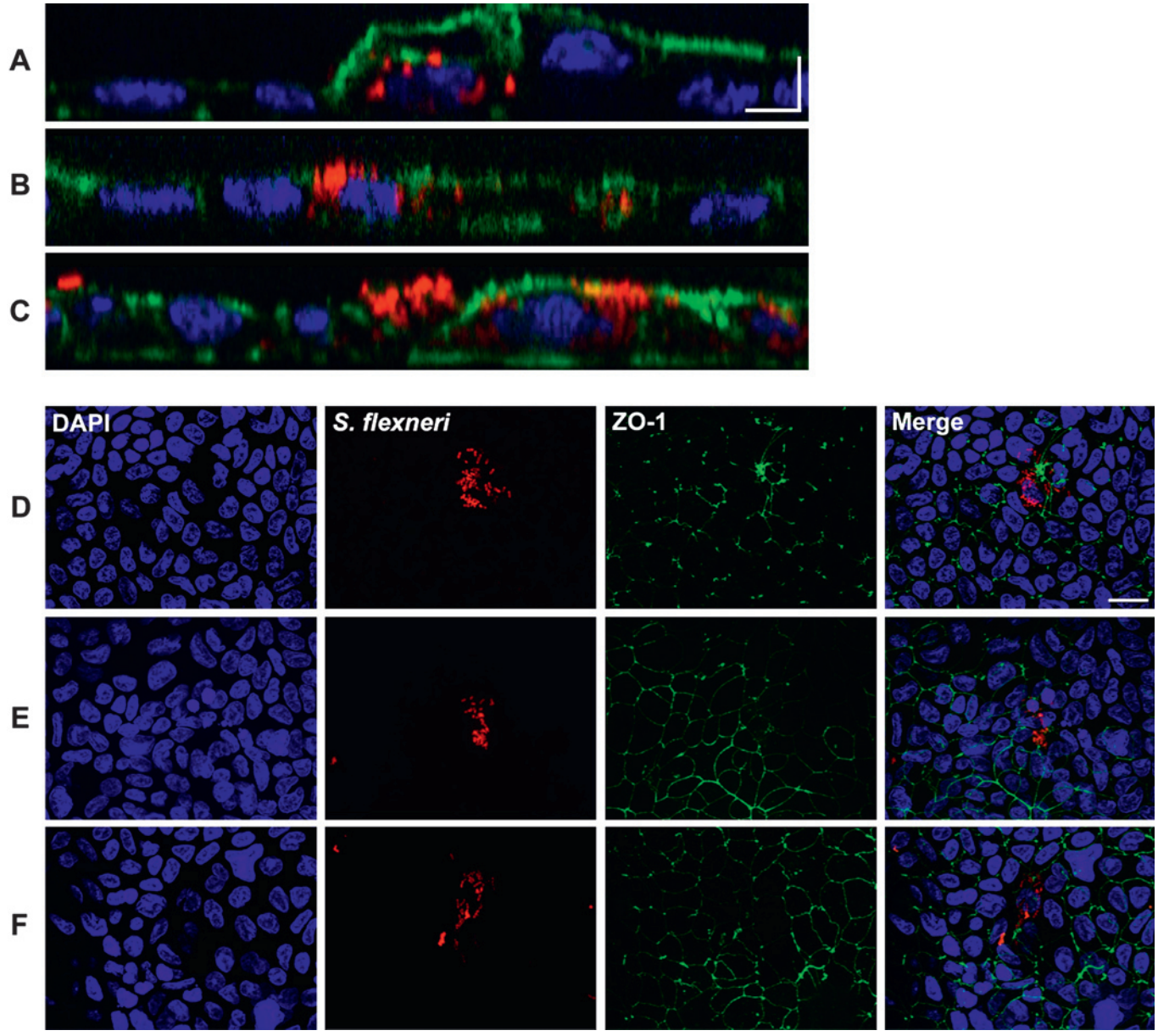

Figure 7 Photomicrographs (along the z-axis) of Caco-2 monolayers infected with *S flexneri* (identified with anti-*S flexneri* antibody (red)) and stained with 4′,6-diamidino-2-phenylindole (DAPI) (blue) and phalloidin/fluorescein isothiocyanate (green). (A) In Caco-2 cells cultured alone, *S flexneri* was localised within the Caco-2 cells. (B,C) In Caco-2 cells cultured with enteric glial cells (EGCs) (B) and *S*-nitrosoglutathione (GSNO) (C), *S flexneri* was localised within the Caco-2 cells and on the surface of Caco-2 monolayers. Scale bars: 10 μm. (D–F) Photomicrographs of Caco-2 monolayers infected with *S flexneri* (red) and stained with DAPI (blue) and ZO-1 antibody (green). After Caco-2 monolayer infection with *S flexneri*, ZO-1 pericellular staining was significantly reduced and disorganised (D) compared with the Caco-2 areas infected with *S flexneri* after coculture with EGCs (E) or GSNO (F) Scale bar: 20 μm.

(MYPT or PAK phosphorylation, respectively). MYPT phosphorylation and RhoA expression were not modulated by GSNO or EGCs in Caco-2 monolayers (data not shown). In contrast, Cdc42 expression was rapidly and significantly reduced in Caco-2 cells after coculture with EGCs or GSNO (50 μM) (figure 8A,B). In parallel, whereas PAK expression remained stable, expression of phospho-PAK was significantly decreased by EGCs and GSNO (figure 8A,C).

GSNO reduces lesions induced by INV+ in human colonic mucosa explants

GSNO (50 μM) significantly reduced the epithelial desquamation induced by INV+ compared with the control (INV +-infected human colonic explants) (figure 9B–D). Similarly to EGC-CM, epithelial height was not as reduced in the presence of GSNO compared with the control (figure 9E). GSNO did not reduce IL-8 secretion in explants infected with INV+ compared with the control (figure 9F). However, in non-infected colonic explants, GSNO significantly reduced IL-8 secretion (figure 9F).

In vivo effect of GSNO in infected rabbit ligated intestinal loops

We finally sought to identify whether GSNO would have protective effects in vivo in a validated animal model, ie, shigellosis induced in rabbit.[19]

In non-infected loops, ileal villus and crypt architecture were normal (figure 10A). GSNO did not modify mucosal architecture in non-infected loops (figure 10D–F). After infection by INV+,

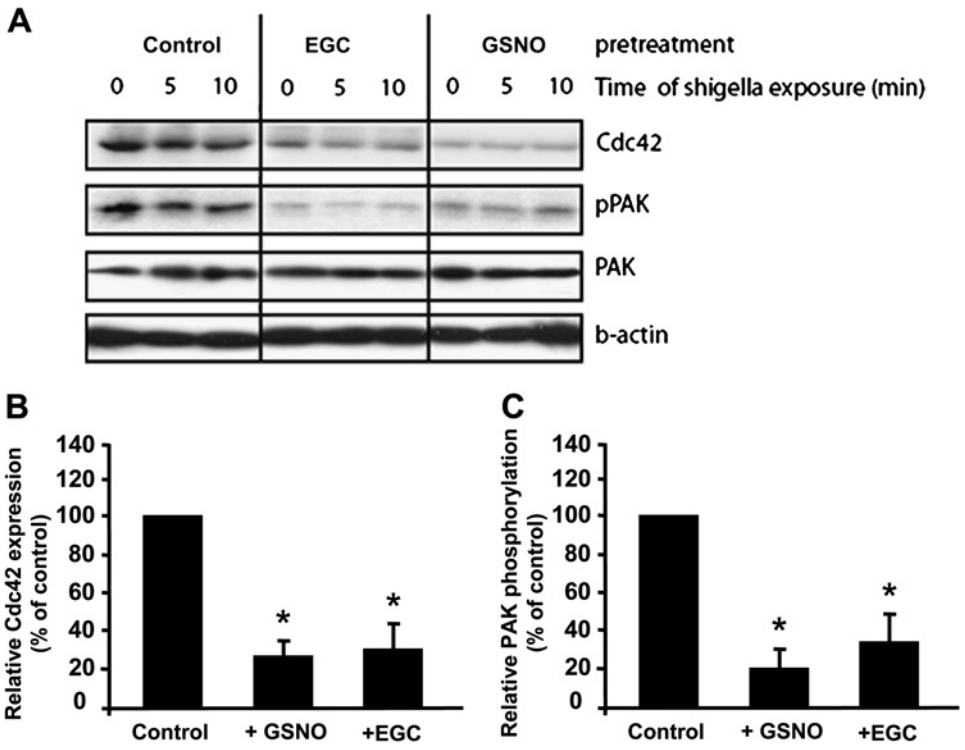

Figure 8 (A,B) Enteric glial cells (EGCs) and *S*-nitrosoglutathione (GSNO; 50μM) inhibit Cdc42 phospho-PAK expression in Caco-2 monolayers. Pretreatment of Caco-2 monolayers for 24 h with EGCs or GSNO induced a significant reduction of Cdc42 expression compared with the control (Caco-2 monolayers cultured alone). (A,C) Consistently, the ratio phospho-PAK/PAK expression was significantly reduced after 24 h coculture with EGCs or GSNO compared with the control. Infection of Caco-2 monolayers by *S flexneri* did not modify the expression of these proteins within the first 10 min after infection independently of the experimental conditions in the epithelial cells (n=3, *p<0.01, pretreated versus control).

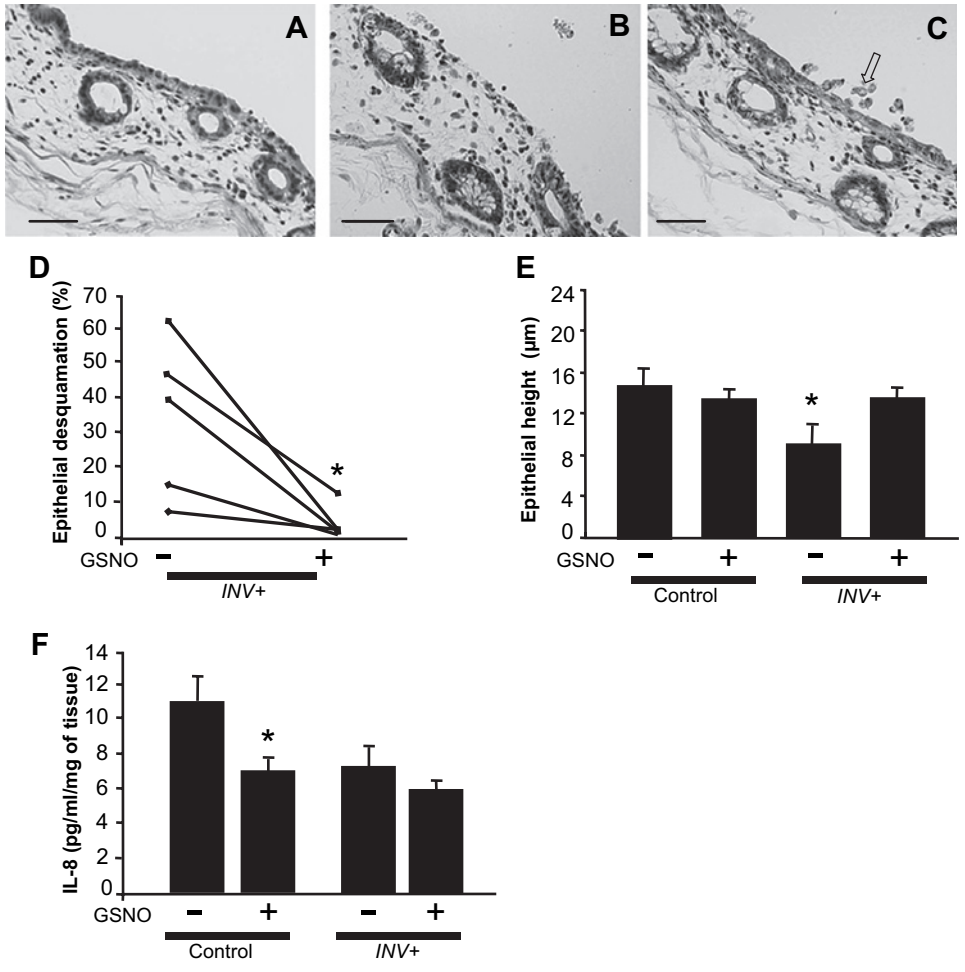

Figure 9 Modulation by *S*-nitrosoglutathione (GSNO) of *S flexneri* effects on barrier morphology and inflammatory response in human colonic explants. (A) No surface epithelium desquamation was observed in control non-infected tissues cultured for 3 h. (B) Infection of the colonic specimen for 3 h with *S flexneri* induced significant desquamation of the surface epithelium. (C) In specimens infected for 3 h with GSNO, moderate desquamation was observed (arrow). Scale bars: 50 μm. (D) Quantitative analysis of epithelial desquamation revealed that GSNO induced a significant decrease in desquamation of the surface epithelium induced by *S flexneri* (INV+) (n=5, *p<0.05). (E) *S flexneri* induced a significant decrease in surface epithelial height compared with the non-infected tissues. GSNO prevented the *S flexneri*-induced decrease in epithelial height (n=5, *p<0.05). (F) GSNO induced a significant decrease in interleukin (IL)-8 secretion compared with the control in non-infected tissue, but not in tissue infected by INV+ (n=5, *p<0.05).

major mucosal damage was observed characterised by a decrease in villus height, an increase in villus diameter and, in some cases, complete destruction of the villus (figure 10B,D–F). In addition, INV+-infected animals also exhibited major PMNL infiltrates in the villus and crypts as well as oedema in the submucosa (figure 10G). Intraperitoneal administration of GSNO significantly reduced the intestinal lesions induced by INV+ (figure 10C–F). In particular, the decrease in villus length to width ratio induced by INV+ was significantly reduced (figure 10D). Similarly, GSNO reduced the percentage of ulcerated villi induced by INV+ (figure 10E). Furthermore, the increase in the submucosa/(submucosa+length of villi and crypt) ratio induced by INV+ was prevented by GSNO (figure 10F). Surprisingly, GSNO treatment increased the PMNL infiltrate induced by INV+ in both the crypts and the villus compartment (figure 10G).

DISCUSSION

In this study, combining ex vivo experiments with human colonic explants and an in vitro coculture model of EGCs and IECs, we first demonstrated that EGCs reduced the IEB lesions and inflammation induced by *S flexneri*. Second, using these models and in vivo models of shigellosis, we identified GSNO as a key glial-derived mediator of these effects.

Previous studies have provided anatomical evidence of a functional role for EGCs in the control of the IEB. Indeed, electron microscopy and immunohistochemical studies revealed a dense network of enteric glia associated with enteric nerve fibres, in close proximity with IECs in both rats and humans.[7 24] From a functional point of view, EGCs have been shown to directly increase IEB resistance and inhibit intestinal epithelial cell proliferation.[7 8] Conversely, glia ablation leads to an increase in cell proliferation and paracellular permeability.[7 8] The present study expands on previous experiments and demonstrates that EGCs exert major protective effects against IEB attack by enteric pathogens. These protective effects were also shown to be cell specific, as fibroblasts did not prevent *S flexneri*-induced IEB lesions.

The protective effects of EGCs on the IEB may be due to the ability of EGCs to prevent the recruitment or degradation by *S flexneri* of key molecular factors necessary for bacterial invasion. EGC protective effects are probably due in part to its ability to inhibit *Shigella* invasion. Indeed, we showed that, after infection, a larger proportion of bacteria were present on the surface of Caco-2 monolayer after treatment with EGCs or GSNO compared with the control, suggesting greater difficulty of INV+ to invade Caco-2 cells. This is further supported at the molecular level by the fact that EGCs decreased Cdc42, a key protein required for *S flexneri* invasion. Indeed, Shibata *et al* have shown that invasion of *S flexneri* was prevented in Cdc42-deficient cells.[25] In addition, the increased expression of ZO-1 induced by EGCs and GSNO in control conditions[8] and during *S flexneri* infection (our study) may also be involved in their protective effects. Indeed, disruption of ZO-1 and other tight junction proteins[26] after *S flexneri* attack could favour bacterial accessibility to the basolateral side of Caco-2 cells and enhance invasion of the monolayer. Besides this mechanism, EGCs have also been shown to increase expression of F-actin.[8] This increased expression of actin polymerisation induced by EGCs may prevent the

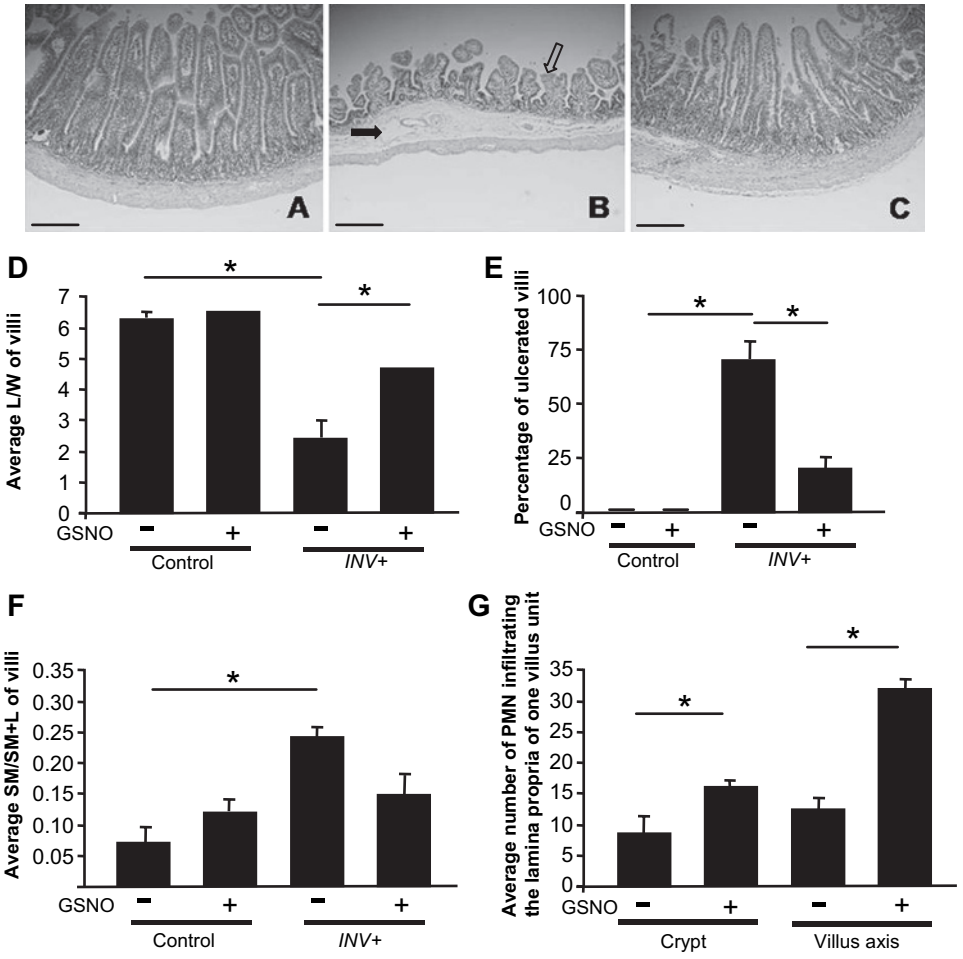

Figure 10 *S*-nitrosoglutathione (GSNO) prevents *S flexneri*-induced barrier lesions in ileal loops in vivo. (A) Normal intestinal mucosa architecture was observed in control loops. (B) Infected intestinal loops showed massive mucosal lesions characterised by oedema (filled arrow), villous atrophy and ulceration (empty arrow). (C) GSNO treatment prevented *S flexneri*-induced lesions. Scale bars: 50 μm. (D) *S flexneri* (INV+) induced a significant reduction in the villus length/width (L/W) ratio. In the presence of GSNO, the L/W ratio was increased compared with the infected non-treated loops (n=6 non-infected loops and 15 infected loops, three rabbits) (*p<0.05). (E) GSNO significantly reduced the percentage of ulcerated villi induced by *S flexneri* (n=6 non-infected loops and 15 infected loops, three rabbits) (*p<0.05). (F) *S flexneri* induced a significant increase in the ratio of submucosa/(submucosa +length of villi and crypt) (SM/SM+L) compared with the non-infected tissues. GSNO prevented the increase in SM/SM +L induced by *S flexneri* (n=6 non-infected loops and 15 infected loops, three rabbits) (*p<0.05). (G) In *S flexneri*-infected loops, GSNO induced a significant increase in polymorphonuclear leucocytes (PMN) in both the crypt and villus axis (n=15 infected loops, three rabbits, *p<0.05).

recruitment of actin by *S flexneri* that is necessary for both its entry into and intracellular motility within IECs.[27]

Our data also suggest that EGCs may reduce IEB lesions via their anti-inflammatory effects, as inflammation has been shown to favour *S flexneri* invasion and spread across the IEB.[28] EGC-mediated inhibition of IL-8 secretion is probably not solely due to reduced monolayer infection. Indeed, for a given area of infected IEB, IL-8 concentration was reduced when IEB was cultured in the presence of EGCs compared with the control. Further reinforcing a direct anti-inflammatory effect of EGCs is the observation that, in non-infected explants of human colonic mucosa, EGC-CM significantly reduced IL-8 concentration compared with the control. Finally, we also demonstrated that the protective effects of EGCs were not associated with an effect on *S flexneri* survival, as (1) culturability of *S flexneri* incubated with EGC-CM (or GSNO) was not modified compared with non-treated bacteria and (2) GSNO tended to increase INV+ invasiveness.

A major finding of this study was the identification of GSNO as a glial-derived mediator involved in the protective effects of EGC. A recent study has identified GSNO as a soluble EGC-derived factor, which increased barrier resistance and reduced paracellular permeability.[8] Consistently, GSNO has been shown to prevent increased paracellular permeability of IEB induced by skin burn.[29] We here extend the role of GSNO to barrier protective effects during bacterial challenge. Indeed, GSNO promoted protection against IEB lesions induced by *S flexneri* in both human explants and an in vivo model of shigellosis. This effect was probably mainly due to its barrier reinforcing properties compared with its anti-inflammatory properties. Indeed, firstly, just pretreatment of Caco-2 with GSNO was sufficient to reduce *S flexneri*-induced IEB lesions. Secondly, in vivo, there was an increased number of PMNLs in the mucosa of GSNO-infected rabbits, suggesting that PMNL recruitment was not prevented by GSNO but that GSNO may have prevented leakage of PMNLs into the lumen through its maintenance of IEB integrity. Surprisingly, GSNO did not modify IL-8 secretion in *S flexneri*-infected human explants. This may be the result of a combined effect of GSNO (1) maintaining the integrity of IEB, the epithelial cells of which are a major source of IL-8,[30] and (2) exerting an anti-inflammatory effect.

GSNO effects are probably not mediated by glutathione alone as reduced glutathione did not prevent *S flexneri*-induced IEB lesions. Several studies have shown that GSNO effects may be mediated by its ability to act as an NO donor.[31] NO has been shown to have a protective effect on the IEB at low concentrations, but a damaging effect at higher ones.[32] Consistently, our data showed that, whereas at 50 μM GSNO had protective effects, at 100 μM it lost its protective effects. Surprisingly, GSNO was only protective when added to the basolateral side of the IEB. This suggests that the ability of GSNO to act as a simple NO donor is probably not involved in its effects, as NO is known to diffuse extremely easily through cell membranes.[33] However, GSNO has been shown to transnitrosylate redox-sensitive protein thiols.[31] Although currently speculative, transnitrosylation by GSNO of key proteins involved in *S flexneri*-mediated effects on IEB—for example, actin and small GTPase—may explain its protective effects. For instance, S-nitrosylation of actin has been shown to prevent its polymerisation in neutrophils[34] and could, if similar phenomena occur in IECs, interfere with *Shigella* entry. Indeed, GSNO-induced actin nitrosylation in IECs would inhibit the invasive process of *S flexneri* by interfering with its ability to recruit actin filaments. An anti-inflammatory effect of GSNO has been demonstrated in our study, which is consistent with data from the literature. Indeed, S-nitrosylated agents such as GSNO have been shown to inhibit synthesis of cytokines such as IL-1β,[35] IL-12p40 subunit,[36] IL-6, IL-8 and MAP[37] and to induce expression of the anti-inflammatory mediators, IRAK-M[38] and SOCS-1.[39] In addition, GSNO effects have been shown to be mediated via attenuation of NF-κB p50-p65 activity by S-nitrosylation of a conserved Cys residue at the NF-κB interface[40] or by S-nitrosylation of the inhibitory-κB (I-κB) kinase, which phosphorylates and promotes the degradation of the NF-κB inhibitory protein I-κB.[41]

Our study lays the basis for further extending the therapeutic potential of GSNO in the treatment of bacterial enteric infection. Beneficial roles for GSNO have been demonstrated in various diseases[41] affecting different organs such as brain,[42] heart[43] and lung.[44] However, to date, no study has demonstrated its potential in gastrointestinal disease except one by Savidge *et al*, showing restoration of colonic permeability in biopsy specimens from patients with Crohn's disease.[8]

In conclusion, our study further highlights a major protective function of EGCs on IEB during an infectious insult. In addition, it lays the scientific basis for the therapeutic use of GSNO to reduce barrier susceptibility to infectious or inflammatory challenge.

Acknowledgements We are grateful to Mr P Hulin and Mrs M Clément (Cellular Imaging Platform PiCell, IFR26, Nantes, France) for the confocal pictures.

Funding MF was supported by a master fellowship from Sanofi-Aventis and was the recipient of an IRMAD Astra-Zeneca grant. Part of this work was also supported by a grant from INCA 'Appel à projets libres 2007'. TS was supported by Eli Broad Foundation and National Institutes of Health (1R21DK078032). M R-D. is funded by the Centre National de la Recherche Scientifique (CNRS).

Competing interests None.

Provenance and peer review Not commissioned; externally peer reviewed.

REFERENCES

1. **Hollander D.** Intestinal permeability, leaky gut, and intestinal disorders. *Curr Gastroenterol Rep* 1999;**1**:410—16.
2. **Balfour Sartor R.** Bacteria in Crohn's disease: mechanisms of inflammation and therapeutic implications. *J Clin Gastroenterol* 2007;**41**(Suppl 1):S37—43.
3. **Arrieta MC,** Madsen K, Doyle J, *et al*. Reducing small intestinal permeability attenuates colitis in the IL10 gene-deficient mouse. *Gut* 2009;**58**:41—8.
4. **Neunlist M,** Toumi F, Oreschkova T, *et al*. Human ENS regulates the intestinal epithelial barrier permeability and a tight junction-associated protein ZO-1 via VIPergic pathways. *Am J Physiol Gastrointest Liver Physiol* 2003;**285**:G1028—36.
5. **Conlin VS,** Wu X, Nguyen C, *et al*. Vasoactive intestinal peptide ameliorates intestinal barrier disruption associated with Citrobacter rodentium-induced colitis. *Am J Physiol Gastrointest Liver Physiol* 2009;**297**:G735—50.
6. **Hoff S,** Zeller F, von Weyhern CW, *et al*. Quantitative assessment of glial cells in the human and guinea pig enteric nervous system with an anti-Sox8/9/10 antibody. *J Comp Neurol* 2008;**509**:356—71.
7. **Neunlist M,** Aubert P, Bonnaud S, *et al*. Enteric glia inhibit intestinal epithelial cell proliferation partly through a TGF-beta1-dependent pathway. *Am J Physiol Gastrointest Liver Physiol* 2007;**292**:G231—41.
8. **Savidge TC,** Newman P, Pothoulakis C, *et al*. Enteric glia regulate intestinal barrier function and inflammation via release of S-nitrosoglutathione. *Gastroenterology* 2007;**132**:1344—58.
9. **Bush TG,** Savidge TC, Freeman TC, *et al*. Fulminant jejuno-ileitis following ablation of enteric glia in adult transgenic mice. *Cell* 1998;**93**:189—201.
10. **Cornet A,** Savidge TC, Cabarrocas J, *et al*. Enterocolitis induced by autoimmune targeting of enteric glial cells. A possible mechanism in Crohn's disease? *Proc Natl Acad Sci U S A* 2001;**98**:13306—11.
11. **Aubé AC,** Cabarrocas J, Bauer J, *et al*. Changes in enteric neurone phenotype and intestinal functions in a transgenic mouse model of enteric glia disruption. *Gut* 2006;**55**:630—7.
12. **Sansonetti PJ.** Shigellosis: an old disease in new clothes? *PLoS Med* 2006;**3**:e354.
13. **Sansonetti PJ,** Tran Van Nhieu G, Egile C. Rupture of the intestinal epithelial barrier and mucosal invasion by *Shigella flexneri*. *Clin Infect Dis* 1999;**28**:466—75.
14. **Philpott DJ,** Yamaoka S, Israel A, *et al*. Invasive *Shigella flexneri* activates NF-kappa B through a lipopolysaccharide-dependent innate intracellular response and leads to IL-8 expression in epithelial cells. *J Immunol* 2000;**165**:903—14.

15. **Coron E,** Flamant M, Aubert P, *et al*. Characterisation of early mucosal and neuronal lesions following *Shigella flexneri* infection in human colon. *PLoS One* 2009;**4**:e4713.
16. **Phalipon A,** Mulard LA, Sansonetti PJ. Vaccination against shigellosis: is the path that is difficult or is it the difficult that is the path? *Microbes Infect* 2008;**10**:1057—62.
17. **Abdo H,** Derkinderen P, Gomes P, *et al*. Enteric glial cells protect neurons from oxidative stress in part via reduced glutathione. *FASEB J* 2010;**24**:1082—94.
18. **Inoue K,** Akaike T, Miyamoto Y, *et al*. Nitrosothiol formation catalyzed by ceruloplasmin. Implication for cytoprotective mechanism in vivo. *J Biol Chem* 1999;**274**:27069—75.
19. **Sansonetti PJ,** Arondel J, Cavaillon JM, *et al*. Role of interleukin-1 in the pathogenesis of experimental shigellosis. *J Clin Invest* 1995;**96**:884—92.
20. **Ruhl A,** Trotter J, Stremmel W. Isolation of enteric glia and establishment of transformed enteroglial cell lines from the myenteric plexus of adult rat. *Neurogastroenterol Motil* 2001;**13**:95—106.
21. **Livak KJ,** Schmittgen TD. Analysis of relative gene expression data using real-time quantitative PCR and the 2(-Delta Delta C(T)) Method. *Methods* 2001;**25**:402—8.
22. **Bulgin RR,** Arbeloa A, Chung JC, *et al*. EspT triggers formation of lamellipodia and membranes ruffles through activation of Rac-1 and Cdc42. *Cell Microbiol* 2009;**11**:217—29.
23. **Demali KA,** Jue AL, Burridge K. IpaA targets beta1 integrins and rho to promote actin cytoskeleton rearrangements necessary for Shigella entry. *J Biol Chem* 2006;**281**:39534—41.
24. **Mestres P,** Diener M, Rummel W. Electron microscopy of the mucosal plexus of the rat colon. *Acta Anat (Basel)* 1992;**143**:275—82.
25. **Shibata T,** Takeshima F, Chen F, *et al*. Cdc42 facilitates invasion but not the actin-based motility of Shigella. *Curr Biol* 2002;**12**:341—5.
26. **Sakaguchi T,** Kohler H, Gu X, *et al*. *Shigella flexneri* regulates tight junction-associated proteins in human intestinal epithelial cells. *Cell Microbiol* 2002;**4**:367—81.
27. **Tran Van Nhieu G,** Bourdet-Sicard R, Dumenil G, *et al*. Bacterial signals and cell responses during Shigella entry into epithelial cells. *Cell Microbiol* 2000;**2**:187—93.
28. **Sansonetti PJ,** Arondel J, Huerre M, *et al*. Interleukin-8 controls bacterial transepithelial translocation at the cost of epithelial destruction in experimental shigellosis. *Infect Immun* 1999;**67**:1471—80.
29. **Costantini TW,** Bansal V, Krzyzaniak MJ, *et al*. Vagal nerve stimulation protects against burn-induced intestinal injury through activation of enteric glia cells. *Am J Physiol Gastrointestinal Liver Physiol* Published Online First: 2010 August 12. doi:10.1152/ajpgi.00156.2010.
30. **Branka JE,** Vallette G, Jarry A, *et al*. Early functional effects of Clostridium difficile toxin A on human colonocytes. *Gastroenterology* 1997;**112**:1887—94.
31. **Gaston BM,** Carver J, Doctor A, *et al*. S-nitrosylation signaling in cell biology. *Mol Interv* 2003;**3**:253—63.
32. **Natal C,** Modol T, Oses-Prieto JA, *et al*. Specific protein nitration in nitric oxide-induced apoptosis of human monocytes. *Apoptosis* 2008;**13**:1356—67.
33. **Arzumanian V,** Stankevicius E, Laukeviciene A, *et al*. [Mechanisms of nitric oxide synthesis and action in cells] (In Lithuanian). *Medicina (Kaunas)* 2003;**39**:535—41.
34. **Thom SR,** Bhopale VM, Mancini DJ, *et al*. Actin S-nitrosylation inhibits neutrophil beta2 integrin function. *J Biol Chem* 2008;**283**:10822—34.
35. **Schroeder RA,** Cai C, Kuo PC. Endotoxin-mediated nitric oxide synthesis inhibits IL-1beta gene transcription in ANA-1 murine macrophages. *Am J Physiol* 1999;**277**:C523—30.
36. **Xiong H,** Zhu C, Li F, *et al*. Inhibition of interleukin-12 p40 transcription and NF-kappaB activation by nitric oxide in murine macrophages and dendritic cells. *J Biol Chem* 2004;**279**:10776—83.
37. **Into T,** Inomata M, Nakashima M, *et al*. Regulation of MyD88-dependent signaling events by S nitrosylation retards toll-like receptor signal transduction and initiation of acute-phase immune responses. *Mol Cell Biol* 2008;**28**:1338—47.
38. **del Fresno C,** Gomez-Garcia L, Caveda L, *et al*. Nitric oxide activates the expression of IRAK-M via the release of TNF-alpha in human monocytes. *Nitric Oxide* 2004;**10**:213—20.
39. **Gonzalez-Leon MC,** Soares-Schanoski A, del Fresno C, *et al*. Nitric oxide induces SOCS-1 expression in human monocytes in a TNF-alpha-dependent manner. *J Endotoxin Res* 2006;**12**:296—306.
40. **Marshall HE,** Stamler JS. Inhibition of NF-kappa B by S-nitrosylation. *Biochemistry* 2001;**40**:1688—93.
41. **Foster MW,** Hess DT, Stamler JS. Protein S-nitrosylation in health and disease: a current perspective. *Trends Mol Med* 2009;**15**:391—404.
42. **Prasad R,** Giri S, Nath N, *et al*. GSNO attenuates EAE disease by S-nitrosylation-mediated modulation of endothelial-monocyte interactions. *Glia* 2007;**55**:65—77.
43. **Rassaf T,** Poll LW, Brouzos P, *et al*. Positive effects of nitric oxide on left ventricular function in humans. *Eur Heart J* 2006;**27**:1699—705.
44. **Snyder AH,** McPherson ME, Hunt JF, *et al*. Acute effects of aerosolized S-nitrosoglutathione in cystic fibrosis. *Am J Respir Crit Care Med* 2002;**165**:922—6.

Enteric glia protect against *Shigella flexneri* invasion in intestinal epithelial cells: a role for *S*-nitrosoglutathione

Mathurin Flamant, Philippe Aubert, Malvyne Rolli-Derkinderen, Arnaud Bourreille, Margarida Ribeiro Neunlist, Maxime M Mahé, Guillaume Meurette, Benoit Marteyn, Tor Savidge, Jean Paul Galmiche, Philippe J Sansonetti and Michel Neunlist

Gut 2011 60: 473-484 originally published online December 7, 2010
doi: 10.1136/gut.2010.229237

Notes